JPE 2-1-7

A Novel Dead-Time Compensation Method using Disturbance Observer

Hyun-Soo Kim, Hyung-Tae Moon, and Myung-Joong Youn*

Dept. of Electrical Engineering & Computer Science, KAIST, Taejon, Korea

ABSTRACT

A new on-line dead-time compensation method for a permanent magnet (PM) synchronous motor drive is proposed. Using a simple disturbance observer without any additional circuit and off-line experimental measurement, disturbance voltages in the synchronous reference *dq* frame caused by the dead time and non-ideal switching characteristics of power devices are estimated in an on-line manner and fed to voltage references in order to compensate the dead-time effects. The proposed method is applied to a PM synchronous motor drive system and implemented by using software of a digital signal processor (DSP) TMS320C31. Simulations and experiments are carried out for this system and the results well demonstrate the effectiveness of the proposed method.

Key Words: dead-time compensation, disturbance observer, PM synchronous motor

1. Introduction

In recent years, due to the development of high speed switching devices such as power transistors and insulated gate bipolar transistors (IGBT's), pulse width modulated (PWM) voltage source inverters (VSI's) are widely used in adjustable speed motor drives.

In a PWM VSI, since a switching device has finite switching times – turn-on time and turn-off time, a dead time should be considered in a PWM gate signal in order to prevent the simultaneous conduction of two switching devices in each leg of the inverter. Since both switching devices in each leg are off during the dead time and the output voltage is dependent on the direction of an output current, these cause a distortion of the inverter output voltage, which is called as *'dead-time effects'*.

Manuscript received December 18, 2001; revised February 19, 2002.

Corresponding Author: mmyoun@ee.kaist.ac.kr, Tel: +82-42-869-3422, Fax: +82-42-869-3410

The distortion of the inverter output voltage affects machine currents, which results in a phase current distortion, torque pulsations, and degradations of control performance [3]-[10].

In order to overcome this problem, various approaches are presented. The one is based on modified PWM gate signals, where these signals are made from either hardware correction circuits [3]-[5] or a software correction circuit in [6]. The other is based on a feedforward approach, where the compensating voltages obtained from current polarities and prescribed values are fed to the voltage references [7]-[10]. Non-ideal switching characteristics of the power device such as finite switching times and voltage drops of switching devices are also considered in some approaches [8][9].

However, the previous approaches can only be implemented by off-line manners. The switching times and voltage drops of the power devices are varied with operating conditions such as the DC link voltage, phase currents, operating frequency, and motor speed [10]. Thus, it is difficult to compensate the dead-time effects perfectly by off-line manners.

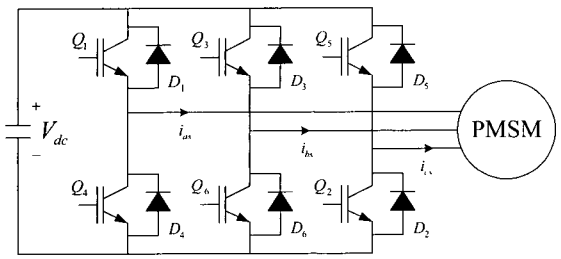

Fig. 1. PM synchronous motor drive system with three-phase PWM VSI.

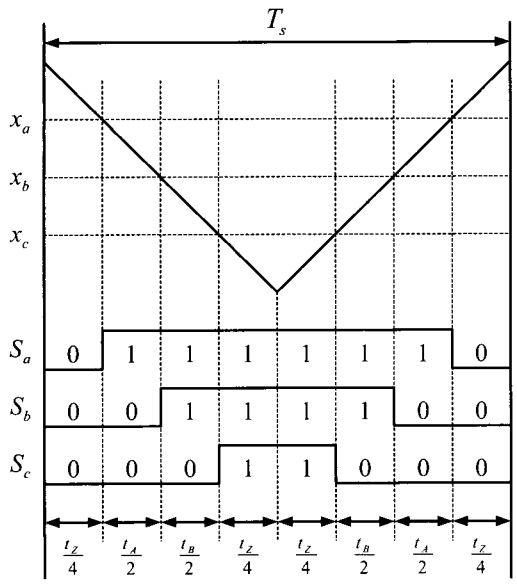

Fig. 2. Ideal gate signal patterns of space vector PWM

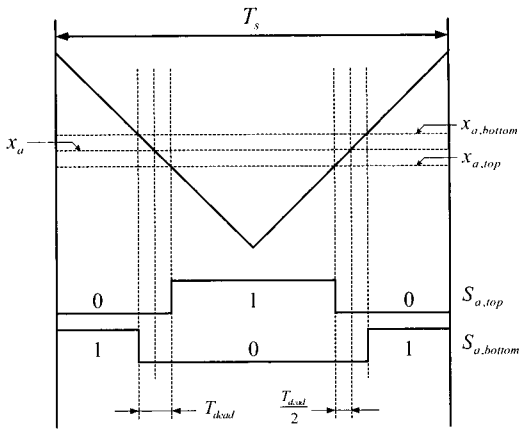

Fig. 3. Practical gate signal patterns considering the dead time.

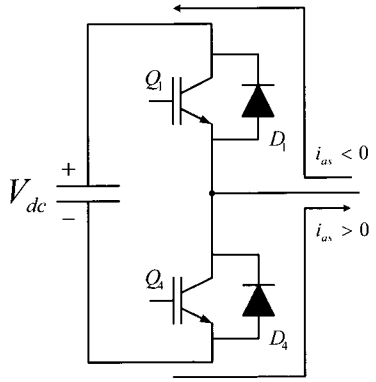

Fig. 4. Basic configuration of one phase leg of PWM inverter.

Although an on-line method is proposed in [10], this method needs additional hardware circuits such as a zero crossing detector and a time counter together with off-line experimental measurements to set up a look-up table.

Thus, in this paper, a new on-line dead-time compensation method using a simple disturbance observer is proposed. The proposed method does not require any additional hardware circuits and off-line experimental measurements. The output voltage errors which are considered as disturbance voltages are estimated by a simple disturbance observer and fed to voltage references in order to compensate the dead-time effects. The proposed method is applied to a PM synchronous motor drive system and implemented in a digital manner using a digital signal processor (DSP) TMS320C31. The simulations and experiments are carried out for this system to show the effectiveness of the proposed method.

2. Analysis of dead-time effects

2.1 Dead-time effects in PWM inverter

A commonly used PM synchronous motor drive systen with a three-phase PWM VSI is shown in Fig. 1. Idea gating signal patterns of the three-phase PWM VSI whic employs the space vector PWM technique are shown i Fig. 2. In practice, however, gate signals of the switchin device are not the same as the ideal signals. Since switching device has a finite switching time, a dead tim should be considered in the PWM gate signals in order t prevent the simultaneous conduction of two switchin devices in each leg of the inverter as shown in Fig. 3. I other words, a top switch of one phase leg should b turned off before a bottom switch of the leg is turned o and vice versa. Although the dead time is very short as few μsecs and guarantees a safe operation of the inverte it adversely causes the performance degradation.

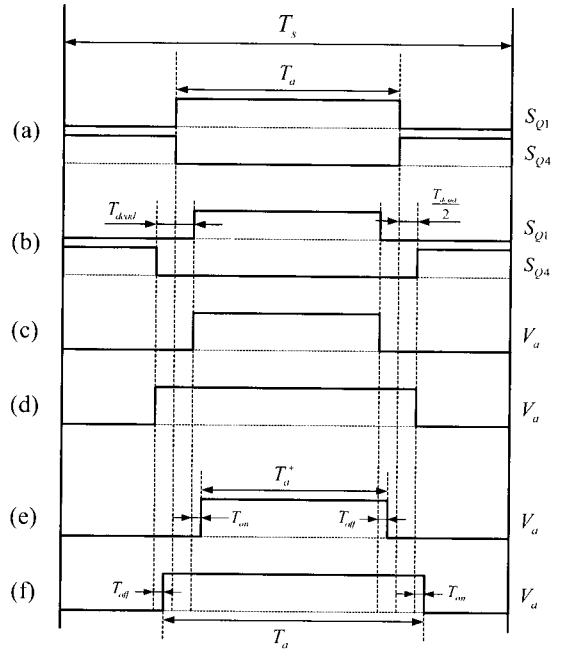

Fig. 5. Practical switching pattern considering the dead time and turn on/off times of switching devices; (a) ideal gate signal patterns (b) practical gate signal pattern considering the dead time (c) actual output voltage considering the dead time for $i_{as} > 0$ (d) actual output voltage considering the dead time for $i_{as} < 0$ (e) actual output voltage considering the dead time and switching time for $i_{as} > 0$ (f) actual output voltage considering the dead time and switching time for $i_{as} < 0$.

It is convenient to analyze the dead-time effects from one phase leg of the inverter and extend the results to the other phase legs. Fig. 4 shows the basic configuration of one phase leg of the PWM inverter, where IGBT's are used as switching devices. During the dead-time period T_{dead}, both the main switching devices Q_1 and Q_4 in the same leg are turned off and the output voltage therefore depends on the direction of the phase current i_{as}. When the gate signal pattern is the same as shown in Fig. 3, the actual output voltages according to the direction of the phase current can be represented as shown in Fig. 5. Fig. 5(a) shows the ideal gate signal pattern and Fig. 5(b) shows the practical gate signal pattern considering the dead time. When the phase current is positive/negative, the phase current flows through the bottom/top diode D_4 / D_1 during the dead-time period. Thus, the switching device in the bottom/top side is considered to be turned on, and Figs. 5(c) and (d) show the output voltages, respectively. The actual phase voltages considering th dead time and switching-time delays are shown in Figs 5(e) and (f). From these figures, the output voltage error caused by the dead time and switching-time delays can b obtained.

When the phase current i_{as} is positive, the turn-on time error $T_{a,err}^+$ and the output voltage error $V_{a,dead}^+$ are calculated from Fig. 5(e) as follows:

$$T_{a,err}^+ = T_a - T_a^+ = T_{dead} + T_{on} - T_{off} \tag{1}$$

$$V_{a,dead}^+ = \frac{T_a - T_a^+}{T_s} V_{dc} \tag{2}$$

where T_a^+ is the effective turn-on time when the phase current is positive.

In a similar way, the turn-on time error and the output voltage error when the phase current i_{as} is negative are represented as follows:

$$T_{a,err}^- = T_a - T_a^- = -\left(T_{dead} + T_{on} - T_{off}\right) \tag{3}$$

$$V_{a,dead}^- = \frac{T_a - T_a^-}{T_s} V_{dc} \tag{4}$$

These equations, therefore, can be summarized as follows:

$$T_{a,err} = \left(T_{dead} + T_{on} - T_{off}\right) \cdot \mathrm{sgn}\left(i_{as}\right) \tag{5}$$

$$V_{a,dead} = \frac{T_{a,err}}{T_s} V_{dc} = V_{dead} \cdot \mathrm{sgn}\left(i_{as}\right) \tag{6}$$

where,

$$\mathrm{sgn}\left(i_{as}\right) = \begin{cases} 1 & : i_{as} > 0 \\ -1 & : i_{as} < 0 \end{cases}, \quad V_{dead} = \frac{T_{dead} + T_{on} - T_{off}}{T_s} \cdot V_{dc}$$

Additionally, the voltage drops of switching device can be considered as follows [9, 10]:

$$V_{dead} = \frac{T_{dead} + T_{on} - T_{off}}{T_s} \cdot \left(V_{dc} - V_{sat} + V_d\right) + \frac{V_{sat} + V_d}{2} \tag{7}$$

where, V_{sat} and V_d are a saturation voltage drop of the active switch and a forward voltage drop of the freewheeling diode, respectively.

In a similar way, the output voltage errors of the other phases can be obtained as follows:

$$V_{b,dead} = \frac{T_{b,err}}{T_s} V_{dc} = V_{dead} \cdot \mathrm{sgn}(i_{bs}) \tag{8}$$

$$V_{c,dead} = \frac{T_{c,err}}{T_s} V_{dc} = V_{dead} \cdot \mathrm{sgn}(i_{cs}) . \tag{9}$$

These output voltage errors can be considered as *'disturbance voltages'* caused by the dead time and switching times.

2.2 Analysis of dead-time effects in the synchronous reference frame

The disturbance voltages in *abc* frame can be transformed to the synchronous reference *dq* frame as follows:

$$\begin{bmatrix} V^r_{q,dead} \\ V^r_{d,dead} \end{bmatrix} = \mathbf{K}^r(\theta_r) \begin{bmatrix} V_{a,dead} \\ V_{b,dead} \\ V_{c,dead} \end{bmatrix} \tag{10}$$

where,

$$\mathbf{K}^r(\theta_r) = \frac{2}{3} \begin{bmatrix} \cos(\theta_r) & \cos\left(\theta_r - \frac{2\pi}{3}\right) & \cos\left(\theta_r + \frac{2\pi}{3}\right) \\ \sin(\theta_r) & \sin\left(\theta_r - \frac{2\pi}{3}\right) & \sin\left(\theta_r + \frac{2\pi}{3}\right) \end{bmatrix}.$$

Also, the phase currents in (6), (8), and (9) can be represented in the *dq* frame as follows:

$$\mathrm{sgn}(i_{as}) = \mathrm{sgn}\left(i^r_{qs} \cos\theta_r + i^r_{ds} \sin\theta_r\right) \tag{11}$$

$$\mathrm{sgn}(i_{bs}) = \mathrm{sgn}\left(i^r_{qs} \cos\left(\theta_r - \frac{2\pi}{3}\right) + i^r_{ds} \sin\left(\theta_r - \frac{2\pi}{3}\right)\right) \tag{12}$$

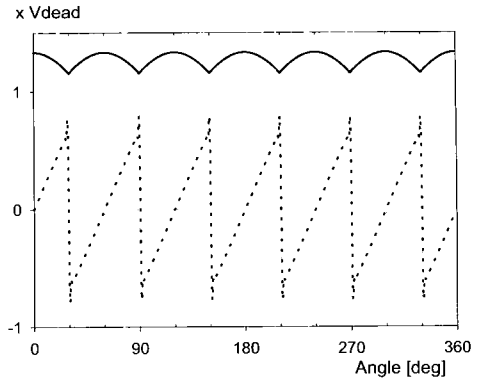

Fig. 6. Disturbance voltages in the synchronous reference frame (Solid line: q-axis disturbance voltage $V^r_{q,dead}$, Dotted line: d-axis disturbance voltage $V^r_{d,dead}$) (*Simulation*).

$$\mathrm{sgn}(i_{cs}) = \mathrm{sgn}\left(i^r_{qs} \cos\left(\theta_r + \frac{2\pi}{3}\right) + i^r_{ds} \sin\left(\theta_r + \frac{2\pi}{3}\right)\right) \tag{13}$$

Using (11) through (13), the disturbance voltages in the synchronous reference frame in (10) can be represented as follows in (14), given at the bottom of the page.

By employing the concept of the field orientation, that is, d axis current i^r_{ds} is controlled to be zero, the disturbance voltages in the synchronous reference frame can be represented in a simpler expression as

$$\begin{bmatrix} V^r_{q,dead} \\ V^r_{d,dead} \end{bmatrix} = V_{dead} \cdot \mathbf{K}^r(\theta_r) \begin{bmatrix} \mathrm{sgn}\left(i^r_{qs} \cos\theta_r\right) \\ \mathrm{sgn}\left(i^r_{qs} \cos\left(\theta_r - \frac{2\pi}{3}\right)\right) \\ \mathrm{sgn}\left(i^r_{qs} \cos\left(\theta_r + \frac{2\pi}{3}\right)\right) \end{bmatrix} \tag{15}$$

Fig. 6 shows disturbance voltages as a function of the electrical position θ_r when i^r_{qs} is positive.

$$\begin{bmatrix} V^r_{q,dead} \\ V^r_{d,dead} \end{bmatrix} = V_{dead} \cdot \mathbf{K}^r(\theta_r) \begin{bmatrix} \mathrm{sgn}\left(i^r_{qs} \cos\theta_r + i^r_{ds} \sin\theta_r\right) \\ \mathrm{sgn}\left(i^r_{qs} \cos\left(\theta_r - \frac{2\pi}{3}\right) + i^r_{ds} \sin\left(\theta_r - \frac{2\pi}{3}\right)\right) \\ \mathrm{sgn}\left(i^r_{qs} \cos\left(\theta_r + \frac{2\pi}{3}\right) + i^r_{ds} \sin\left(\theta_r + \frac{2\pi}{3}\right)\right) \end{bmatrix}. \tag{14}$$

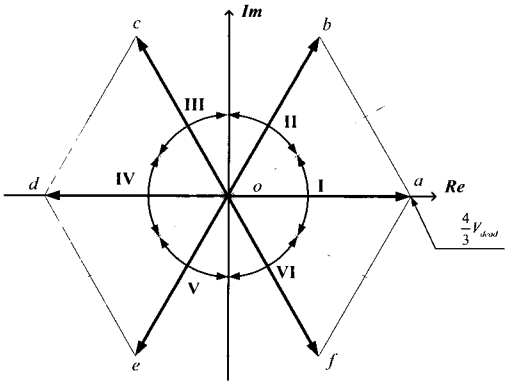

Fig. 7. Disturbance voltages vector according to electrical position.

Table 1. Disturbance voltage vector according to electrical position.

Region	Electrical position	Disturbance voltage vector
I	$-30° < \theta_r < 30°$	$\mathbf{V}_{dead} = \overrightarrow{oa}$
II	$30° < \theta_r < 90°$	$\mathbf{V}_{dead} = \overrightarrow{ob}$
III	$90° < \theta_r < 150°$	$\mathbf{V}_{dead} = \overrightarrow{oc}$
IV	$150° < \theta_r < 210°$	$\mathbf{V}_{dead} = \overrightarrow{od}$
V	$210° < \theta_r < 270°$	$\mathbf{V}_{dead} = \overrightarrow{oe}$
VI	$270° < \theta_r < 330°$	$\mathbf{V}_{dead} = \overrightarrow{of}$

The magnitude of the disturbance voltages in the synchronous reference frame is a function of V_{dead} in (7). While the dead time is a fixed value in general, the switching times of the switching devices are not fixed values but varying with the operating conditions such as the DC link voltage and currents. Moreover, the voltage drops of the switching devices are also varying with the operating conditions. Thus, the magnitude of the disturbance voltages can be considered as a time varying value depending on the operating conditions.

2.3 Analysis of dead-time effects in the stationary reference frame

The disturbance voltages in *abc* frame which are represented in (6), (8), and (9) can be transformed to the stationary reference *dq* frame as follows:

$$\begin{bmatrix} V^s_{q,dead} \\ V^s_{d,dead} \end{bmatrix} = \mathbf{K^s} \begin{bmatrix} V_{a,dead} \\ V_{b,dead} \\ V_{c,dead} \end{bmatrix} = V_{dead} \cdot \mathbf{K^s} \begin{bmatrix} \mathrm{sgn}(i_{as}) \\ \mathrm{sgn}(i_{bs}) \\ \mathrm{sgn}(i_{cs}) \end{bmatrix} \quad (16)$$

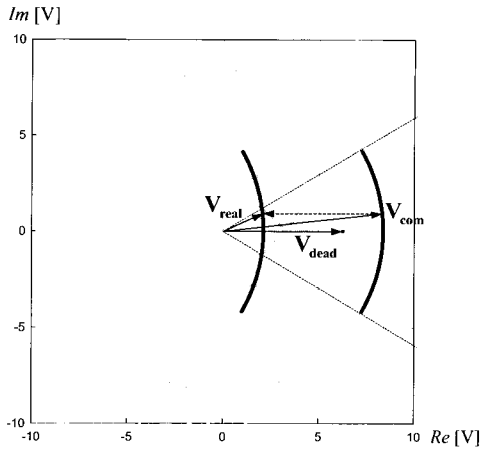

(a)

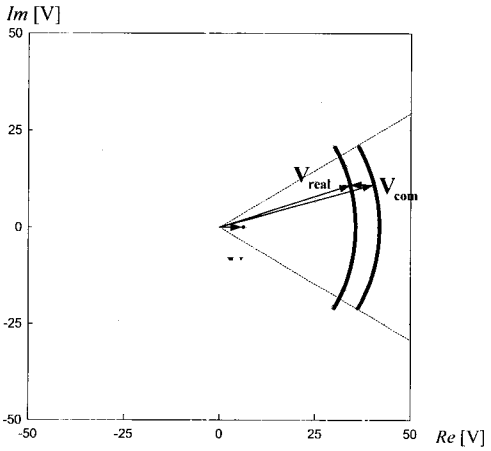

(b)

Fig. 8. Output voltage distortions; (a) at low speed range (@300 [rpm]) (b) at high speed range (@1500 [rpm]).

In the steady state, by employing the concept of the field orientation, (16) can be represented as follows:

$$\begin{bmatrix} V^s_{q,dead} \\ V^s_{d,dead} \end{bmatrix} = V_{dead} \cdot \mathbf{K^s} \begin{bmatrix} \mathrm{sgn}\left(i^r_{qs}\cos(\theta_r)\right) \\ \mathrm{sgn}\left(i^r_{qs}\cos\left(\theta_r - \frac{2\pi}{3}\right)\right) \\ \mathrm{sgn}\left(i^r_{qs}\cos\left(\theta_r + \frac{2\pi}{3}\right)\right) \end{bmatrix} \quad (17)$$

where,

$$\mathbf{K^s} = \frac{2}{3}\begin{bmatrix} \cos(0) & \cos\left(-\frac{2\pi}{3}\right) & \cos\left(\frac{2\pi}{3}\right) \\ \sin(0) & \sin\left(-\frac{2\pi}{3}\right) & \sin\left(\frac{2\pi}{3}\right) \end{bmatrix}$$

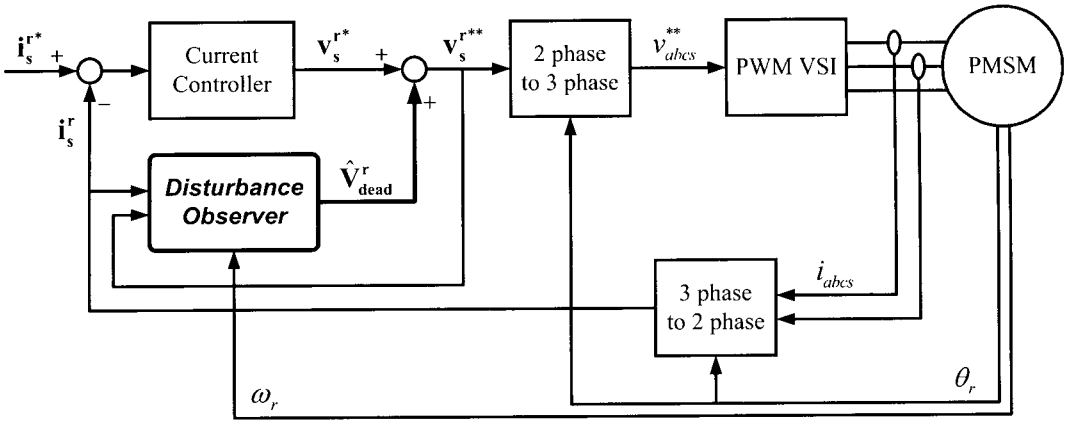

Fig. 9. Block diagram of the proposed dead-time compensation method.

From (17), the disturbance voltage vector in the stationary reference frame can be represented in a space vector as follows:

$$\mathbf{V}^{s}_{dead} = V^{s}_{q,dead} + jV^{s}_{d,dead} \tag{18}$$

From (17) and (18), the disturbance voltage vector can be separated into six vectors according to the electrical position as shown in Table 1, and Fig. 7 shows this voltage vector in the stationary reference frame when i^{r}_{qs} is positive. The magnitude of the disturbance voltage vector is dependent only on the dead-time, switching-time delays, and voltage drops of switching devices, not on the motor speed and voltage reference so that the effect of the disturbance voltage at a low speed range is severer than that at a high speed range as shown in Fig. 8.

3. Estimation and compensation of dead-time effect

The disturbance voltages due to the dead-time effects cause the inverter output voltage distortion, which results in the phase current distortion and torque ripple. Moreover, the magnitude of the disturbance voltages in (15) is a function of a dead time, switching-time delays, voltage drops of switching devices, and a DC link voltage. While the dead time is a fixed value and the DC link voltage can be measured, the switching-time delays and voltage drops of the switching devices are varying with the operating conditions. Since it is very difficult to measure the switching-time delays and voltage drops, the perfect dead-time compensation in an off-line manner is not easy.

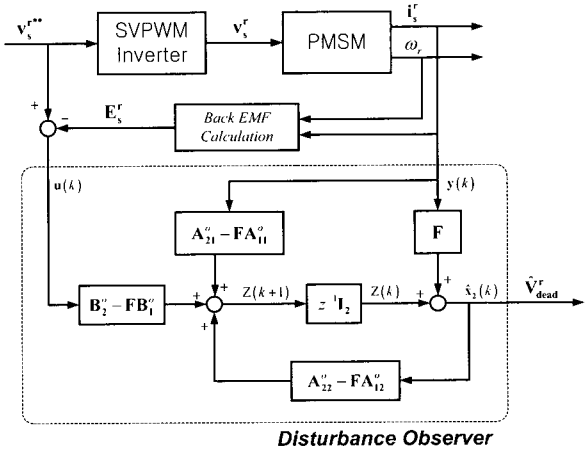

Fig. 10. Block diagram of disturbance voltage observer.

To overcome the above problems, a new on-line dead time compensation method is proposed. The propose method consists of a simple disturbance observer and feedforward loop, and does not require any addition hardware circuits and off-line experimental measurement The disturbance voltages in the synchronous referenc frame are estimated by a disturbance voltage observe which is based on the electrical model of the PM synchronous motor. And the estimated disturbanc voltages are fed to voltage references in order t compensate the dead-time effects as shown in Fig. 9. Fi 10 shows the disturbance voltage observer based on simple state observer.

The electrical modeling of the PM synchronous mot including the disturbance voltages due to the dead-tim effects is represented as follows:

$$\mathbf{v}^{r**}_{s} = \mathbf{r}_{s}\mathbf{i}^{r}_{s} + \mathbf{L}_{s}\frac{d}{dt}\mathbf{i}^{r}_{s} + \mathbf{E}^{r}_{s} + \mathbf{V}^{r}_{dead} \tag{19}$$

where,

$\mathbf{v}_s^{r**} = \begin{bmatrix} v_{ds}^{r**} & v_{qs}^{r**} \end{bmatrix}^T$, $\mathbf{i}_s^r = \begin{bmatrix} i_{ds}^r & i_{qs}^r \end{bmatrix}^T$,

$\mathbf{V}_{dead}^r = \begin{bmatrix} V_{d,dead}^r & V_{q,dead}^r \end{bmatrix}^T$, and $\mathbf{E}_s^r$ is the back EMF vector including decoupling terms and represented as follows:

$$\mathbf{E}_s^r = \begin{bmatrix} -L_q i_{qs}^r \omega_r \\ L_d i_{ds}^r \omega_r + \lambda_m \omega_r \end{bmatrix}$$

Since the sampling period is 150 μsec which is very short, the variation of the disturbance voltages during one sampling period can be assumed as zero, that is,

$$\mathbf{V}_{dead}^r(k+1) = \mathbf{V}_{dead}^r(k) \tag{20}$$

Under the above assumption, the modeling equations of the motor in (19) can be expressed as discrete state equations as follows:

$$\begin{pmatrix} \mathbf{x}_1(k+1) \\ \mathbf{x}_2(k+1) \end{pmatrix} = \begin{pmatrix} \mathbf{A}_{11} & \mathbf{A}_{12} \\ \mathbf{A}_{21} & \mathbf{A}_{22} \end{pmatrix} \begin{pmatrix} \mathbf{x}_1(k) \\ \mathbf{x}_2(k) \end{pmatrix} + \begin{pmatrix} \mathbf{B}_1 \\ \mathbf{B}_2 \end{pmatrix} \mathbf{u}(k) \tag{21}$$

$$\mathbf{y}(k) = \begin{pmatrix} \mathbf{C}_1 & \mathbf{0}_2 \end{pmatrix} \begin{pmatrix} \mathbf{x}_1(k) \\ \mathbf{x}_2(k) \end{pmatrix} \tag{22}$$

where,

$\mathbf{x}_1(k) = \mathbf{i}_s^r(k)$, $\mathbf{x}_2(k) = \mathbf{V}_{dead}^r(k)$,

$\mathbf{u}(k) = \left[\mathbf{v}_s^{r**}(k) - \mathbf{E}_s^r(k) \right]$,

$\mathbf{A}_{11} = \mathbf{I}_2 - T_s \mathbf{L}_s^{-1} \mathbf{R}_s$, $\mathbf{A}_{12} = -T_s \mathbf{L}_s^{-1}$, $\mathbf{A}_{21} = \mathbf{0}_2$, $\mathbf{A}_{22} = \mathbf{I}_2$,

$\mathbf{B}_1 = T_s \mathbf{L}_s^{-1}$, $\mathbf{B}_2 = \mathbf{0}_2$, $\mathbf{C}_1 = \mathbf{I}_2$,

$\mathbf{I}_2 = \begin{bmatrix} 1 & 0 \\ 0 & 1 \end{bmatrix}$, $\mathbf{0}_2 = \begin{bmatrix} 0 & 0 \\ 0 & 0 \end{bmatrix}$, and T_s is a sampling period.

According to the above state equations, the reduced order disturbance voltage observer can be obtained as [2]

$$\hat{\mathbf{x}}_2(k) = Z(k) + \mathbf{F}\mathbf{y}(k) \tag{23}$$

$$Z(k+1) = \bar{\mathbf{A}} Z(k) + \bar{\mathbf{B}} \mathbf{u}(k) + \bar{\mathbf{K}} \mathbf{y}(k) \tag{24}$$

where, $\bar{\mathbf{A}} = \mathbf{A}_{22}^o - \mathbf{F}\mathbf{A}_{12}^o$, $\bar{\mathbf{B}} = \mathbf{B}_2^o - \mathbf{F}\mathbf{B}_1^o$,

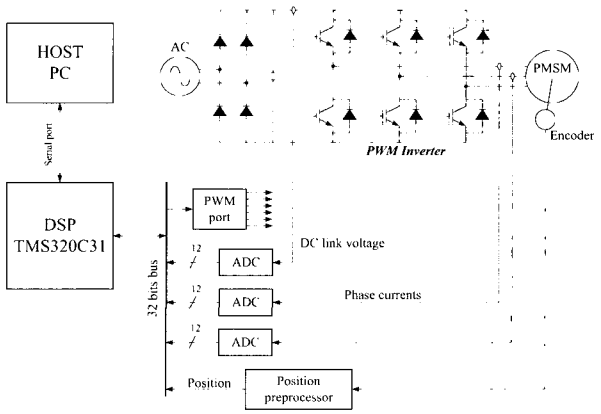

Fig. 11. Configuration of DSP-based control system for PM synchronous motor.

$\bar{\mathbf{K}} = \left(\mathbf{A}_{22}^o - \mathbf{F}\mathbf{A}_{12}^o \right) \mathbf{F} + \left(\mathbf{A}_{21}^o - \mathbf{F}\mathbf{A}_{11}^o \right)$, and $Z(k)$ is a virtual vector, $\mathbf{F}$ is an observer gain matrix, and superscript '^{o}' denotes a nominal value.

Considering the necessary condition for the stable observer, the error dynamics is obtained as follows:

$$\begin{aligned} \mathbf{e}(k+1) &= \hat{\mathbf{x}}_2(k+1) - \mathbf{x}_2(k+1) \\ &= \bar{\mathbf{A}} \left(\hat{\mathbf{x}}_2(k) - \mathbf{x}_2(k) \right) = \bar{\mathbf{A}} \mathbf{e}(k) \end{aligned} \tag{25}$$

where, $\mathbf{e}(k) = \begin{bmatrix} e_{ds}(k) & e_{qs}(k) \end{bmatrix}^T$. Equation (25) shows that the eigenvalues of $\bar{\mathbf{A}}$ determine the behavior of the observer. In order to make the error dynamics of the *d*-axis and *q*-axis in (25) independent and identical each other, the observer gain matrix can be set as follows:

$$\mathbf{F} = F\mathbf{I}_2$$

Then, the matrix $\bar{\mathbf{A}}$ has a double eigenvalue λ as follows:

$$\lambda = 1 + T_s F L_{dqs}^{-1}, \quad (0 \le \lambda < 1) \tag{26}$$

which is the necessary condition for the stable observer.

4. Simulation and experiments

The proposed compensation method is realized using a DSP-based control system of the PM synchronous motor as shown in Fig. 11. The processor is the floating-point DSP (TMS320C31) with a clock of 33MHz.

Table 2. Specifications of experimental system.

DC link voltage	310 [V]
Switching period	150 [μsec]
Dead-time	3.6 [μsec]
Switching device	PM50RSA060
Turn-on time*	0.8-2.0 [μsec]
Turn-off time*	2.0-2.9 [μsec]
Saturation voltage*	1.8-2.7 [V]
Diode forward voltage*	2.2-3.3 [V]

* : Mitsubishi data book

Table 3. Specifications of test motor.

Motor type	PMSM
Number of poles	8
Rated power	750 [W]
Rated speed	3000 [rpm]
Rated torque	2.4 [Nm]
Rated current	6.0 [A]
Stator resistance	0.49 [Ω]
Stator inductance	6.9 [mH]
Linkage flux	0.0667 [Wb]
Position sensor	Absolute encoder (11b/r)

Hall effect devices are used to measure phase currents and a DC link voltage, and the measured signals are converted to digital values by using analog-to-digital converters (ADC's) with a resolution of 12 bits. An absolute encoder with a resolution of 11-bit/rev and a position preprocessor are employed to obtain the position information on the rotor. The three-phase PWM inverter is constructed by using the intelligent power module (PM50RSA060; Mistubishi), gate drives, and protection circuits. The sampling period and switching period of the system are set to 150 μsec and an 8-pole PM synchronous motor is used for the test motor. The other specifications of the experimental system and test motor are shown in Tables 2 and 3, respectively.

4.1 Determination of observer gains

The gain of the disturbance voltage observer is determined using the values of the experimental system and test motor. From the necessary condition for th stability in (26), the stable range of the observer gain ca be calculated as follows:

$$-69 \le F < 0 \qquad (27)$$

The deadbeat performance is possible by letting $\lambda =$ in (26). This corresponds to the deadbeat gain c $F_0 = -69$. However, it is difficult to realize the deadbe gain F_0 in the actual system because noises involved i the detected currents would be amplified in th disturbance observer. The disturbance observer of th continuous model can be regarded as a first-order low pa filter whose bandwidth is determined by an observer gai If the eigenvalue λ approaches to 0, the stability cann be guaranteed while the time delay of the observer decreased, and vice versa. Thus, the observer gain shoul be determined by taking account of a trade off between th stability and the time delay of the observer. In this pape the observer gain is determined as $F = -27.6$, that i $\lambda = 0.6$. The time delay of the disturbance observer about 700 μsec under the above observer gain and th time delay is fast enough to estimate the disturbanc voltages.

4.2 Simulation results

To show the effectiveness of the proposed method, th simulations are carried out in the PM synchronous mot drive system. Fig. 12 shows the simulation results of th current control with/without a dead-time compensatio using the proposed method, where the q-axis and d-ax current references are given as 3A (half the rated valu and 0A, respectively, and the motor is operated at 150rp (electrically 10Hz). The current controllers of bo schemes are PI current controllers in the synchrono reference frame.

Without a dead-time compensation scheme, the pha current is distorted severely due to the dead-time effects shown in Fig. 12(a). However, this distortion remarkably reduced in the proposed scheme as shown i Fig. 12(b). Figs. 12(c) and (d) show the dq-axis curre waveforms and the spectra in both schemes, respectivel It can be also shown that the current pulsations and the harmonics are reduced in the proposed scheme as show in Fig. 12(d).

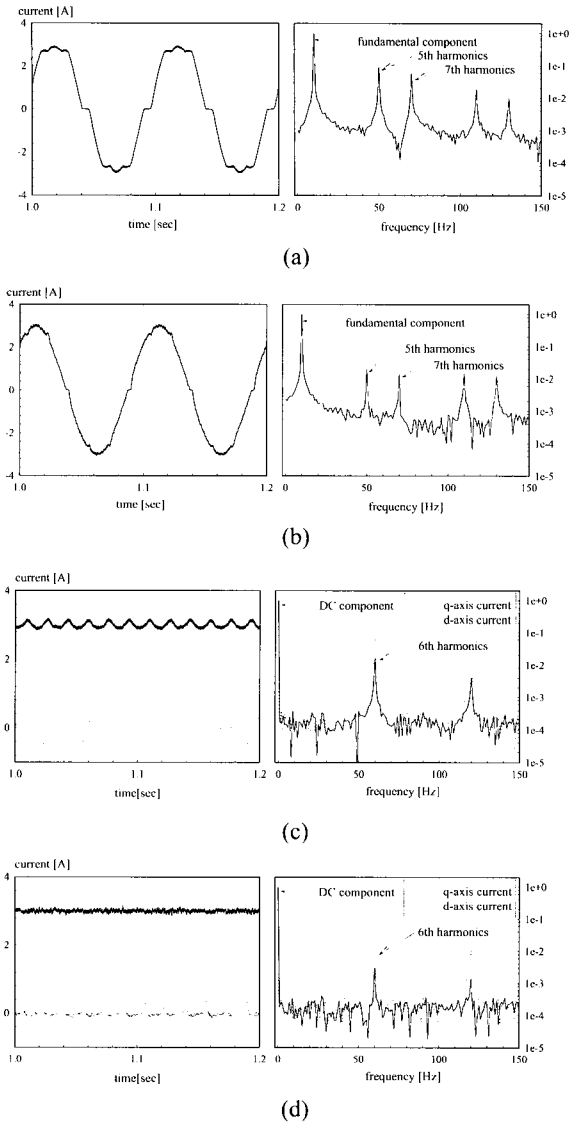

Fig 12. Simulation results of current control; (a) phase current without dead time compensation (b) phase current with dead time compensation using proposed method (c) dq-axis current without dead time compensation (d) dq-axis current with dead time compensation using proposed method.

The current ripple ratio (CRR) and total harmonic distortion (THD) of the q-axis current are compared with each other. The current ripple ratio is defined as the ratio of a current ripple variation to the rated current of the motor in steady state as follows:

$$CRR = \frac{\Delta i_q^r}{i_{rated}} \tag{28}$$

The total harmonic distortion for present purpose is defined as

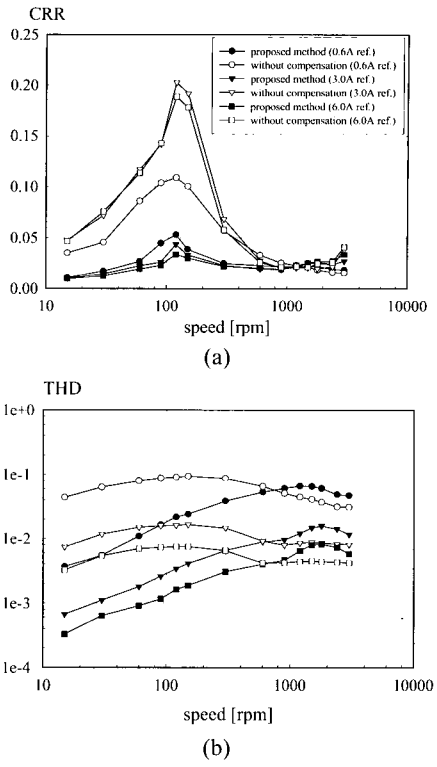

Fig. 13. Characteristics of current ripple ratio and total harmonic distortion of q-axis current *(Simulation results)*; (a) current ripple ratio (b) total harmonic distortion.

$$THD = \left(\sqrt{\sum_{n=1}^{15} i_{qn}^{r\,2}} \right) \Big/ i_{q0}^r \tag{29}$$

where, i_{q0}^r and i_{qn}^r are the DC component and n-th order harmonic component of the q-axis current, respectively.

The current ripple ratio and the total harmonic distortion of the current control without a compensation scheme are maximum at about 150rpm (electrically 10Hz) as shown in Fig. 13. The bandwidth of the current controller is wide enough to reduce the current distortion at a low speed range (i.e. below tens rpm). At a high speed range (i.e. over hundreds rpm), although the current controller cannot reduce the distortion, the ratio of the magnitude of the disturbance voltage vector to that of the reference voltage vector decreases as the motor speed increases.

4.3 Experimental results

Fig. 14 shows the estimated dq-axis disturbance voltages in the synchronous reference frame when the

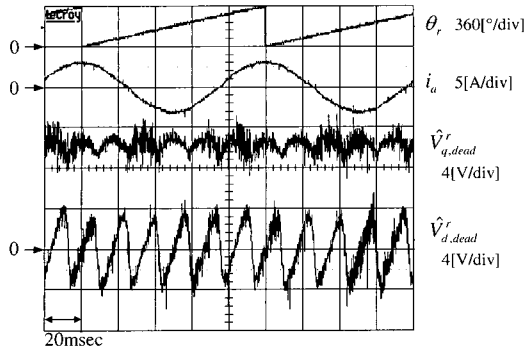

Fig. 14. Estimation of disturbance voltages using disturbance observer *(Experimental results)*.

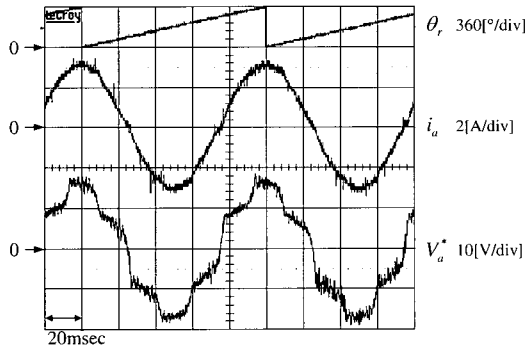

Fig. 15. Phase voltage reference (Experimental results).

motor is operated at 150 rpm. The estimated disturbance voltages show nearly the same waveforms as the simulation results as shown in Fig. 6, although the levels of the estimated disturbance voltages are somewhat different from the simulation results. This is due to the operating condition of the PWM inverter. A phase current waveform and a phase voltage reference using the proposed method with a dead-time compensation are shown in Fig. 15. The reference voltage has been modified in order to compensate the dead-time effects.

In order to show the validity of the proposed method, some experiments are carried out. In these experiments, the motor is operated at 150 rpm with a constant current reference of 3A. The performance of the current controller with the proposed dead-time compensation scheme is compared with those of the no compensation scheme and the off-line compensation scheme, where the off-line scheme means the current controller with the Sukegawa dead-time compensation scheme which is an off-line feedforward dead-time compensation method [7].

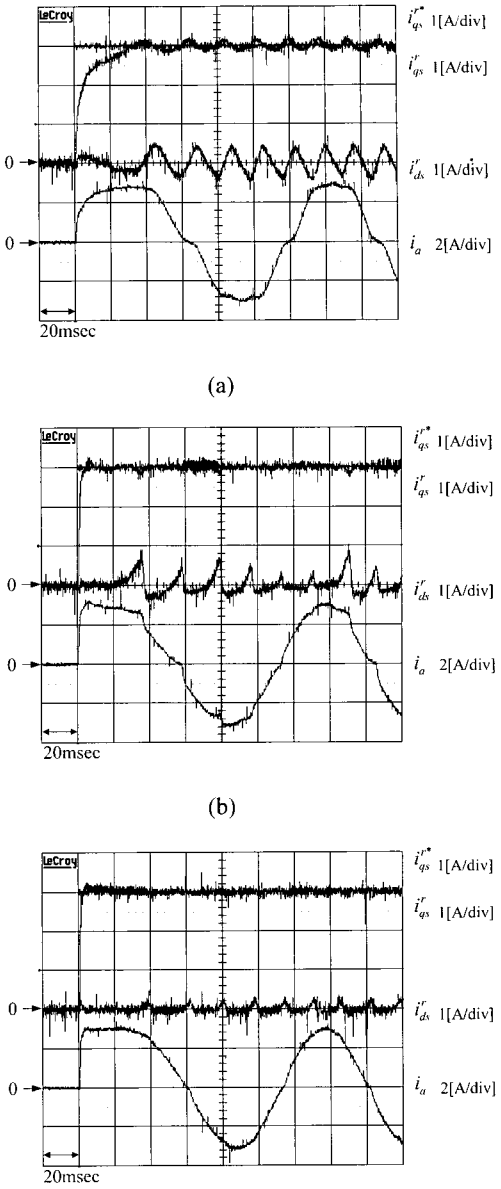

Fig. 16. Step response of current control *(Experimental results* (a) without dead time compensation (b) with dead-tin compensation using Sukegawa method[7] (c) with dead-tin compensation using proposed method.

Fig. 16 shows the *dq*-axis current waveforms of thre schemes for the step change of the current referenc e (d axis current: 0 → 3A). Without a compensation schem the dead time causes the undesired current pulsation s c about six times the electrica l fre ency in the *dq*-ax currents and the distortion in the phase current as shown Fig. 16(a).

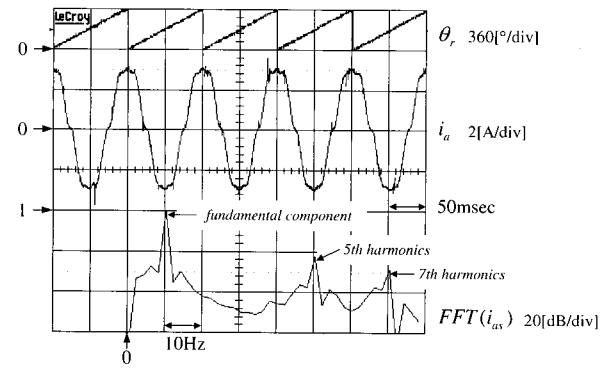

(a)

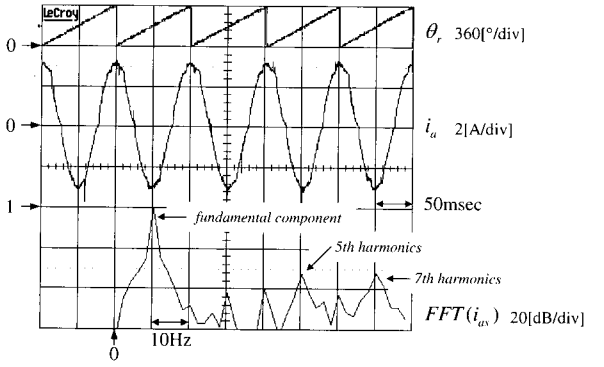

(b)

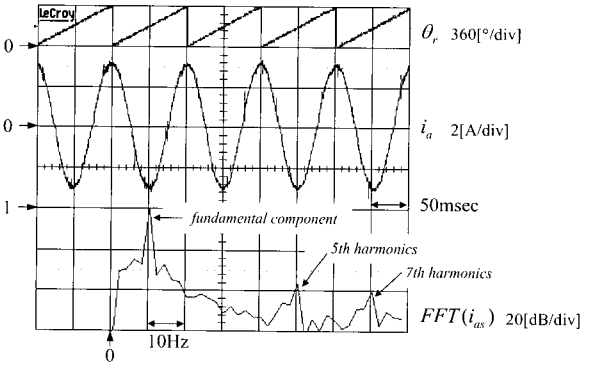

(c)

Fig. 17. Phase current waveforms and spectra *(Experimental results)*; (a) without dead time compensation (b) with dead-time compensation using Sukegawa method[7] (c) with dead-time compensation using proposed method.

Moreover, the dynamic behavior of the current control is very slow, i.e., over 20msec. In the off-line compensation scheme, although the q-axis current pulsations are remarkably reduced and the dynamic behavior becomes fast, the pulsations in the d-axis current and the distortion in the phase current still exist as shown in Fig. 16(b). However, in the proposed scheme, these are removed perfectly as shown in Fig. 16(c).

The phase current waveforms and their spectra when the motor is operated at steady state are shown in Fig.17. The phase current has less 5th and 7th harmonics components in the proposed scheme as shown in Fig. 17(c) than in the no compensation scheme or in the off-line compensation scheme as shown in Figs. 17(a) or (b), respectively.

5. Conclusions

A new on-line dead-time effects compensation method is proposed. The previous approaches are based on the additional hardware circuits or off-line experimental measurements. However, the magnitude of the disturbance voltage is varying with the operating condition and an on-line measurement of this magnitude is very difficult. The proposed method compensates in an on-line manner the effects caused by the dead-time and non-ideal switching characteristics of the power devices without additional circuits and off-line experiments. The disturbance voltages are estimated by using a simple disturbance observer and fed to the voltage references.

To show the effectiveness of the proposed scheme, the simulations and experiments are carried out in the PM synchronous motor drive system. The simulation and experimental results show a better performance of the proposed method and verify its validity. The proposed method can be applied to the high precision PM synchronous motor drive system.

References

[1] P. C. Krause, *Analysis of Electric Machinery*, McGraw-Hill, New York, 1986.

[2] K. Ogata, *Discrete-Time Control Systems*, Englewood Cliffs, NJ: Prentice-Hall, 1987.

[3] Y. Murai, T. Watanabe, and H. Iwasaki, "Waveform distortion and correction circuit for PWM inverter with switching lag-times", *IEEE Trans. Industry Applications*, vol. IA-23, no. 5, pp. 881~886, Sep./Oct. 1987.

[4] R.C. Dodson, P.D. Evans, H.T. Yazdi, and S.C. Harley, "Compensating for dead time degradation of PWM inverter waveforms", *IEE Proceedings*, vol. 137, pt. B, no. 2, March 1990.

[5] S. G. Jeong and M. H. Park, "The analysis and compensation of dead-time effects in PWM inverters", *IEEE Trans. Industrial Electronics*, vol. 38, no. 2, pp. 108 ~ 114, April 1991.

[6] D. Leggate and R. J. Kerkman, "Pulse-based dead-time compensator for PWM voltage inverter", *IEEE Trans. Industrial Electronics*, vol. 44, no. 2, pp. 191 ~ 197, April 1997.

[7] T. Sukegawa, K. Kamiyama, K. Mizuno, T. Matsui, and T. Okuyama, "Fully digital, vector-controlled PWM VSI-fed ac drives with an inverter dead-time compensation strategy", *IEEE Trans. Industry Applications*, vol. 27, no. 3, pp. 552 ~ 559, May/June 1991.

[8] J. W. Choi and S.K Sul, "A new compensation strategy reducing voltage/current distortion in PWM VSI systems operating with low output voltage", *IEEE Trans. Industry Applications*, vol. 31, no. 5, pp. 1001 ~ 1008, Sep./Oct. 1995.

[9] J. W. Choi and S.K Sul, "Inverter output voltage synthesis using novel dead-time compensation", *IEEE Trans. Power Electronics*, vol. 11, no. 2, pp. 221 ~ 227, March 1996.

[10] A. Munoz-Garcia and T. A. Lipo, "On-line dead-time compensation technique for open-loop PWM-VSI drives", *IEEE Appli. Power Elect. Conf Rec.*, pp. 95 ~ 100, Feb. 1998.

Hyun-Soo Kim was born in Kyungpook, Korea, in 1972. He received the B.S. and M. S. degrees in electrical engineering from the Korea Advanced Institute of Science and Technology (KAIST), Deajeon, Korea, in 1994 and 1996, respectively. He is currently working toward the PH. D. degree in electrical engineering at KAIST. His research interests are in the areas on power electronics and control, which include ac machine drives and microprocessor-based control applications.

Hyung-Tae Moon was born in Kwang-Ju Korea, in 1967. He received the B.S. degre in electrical engineering from Kore University, Seoul, Korea, in 1990, and th M.S. degree in electrical engineering fror the Korea Advanced Institute of Science an Technology (KAIST), Daeieon, Korea, i 1993. From 1993 until now, he is a Research Engineer in Mand R&D Center, where was engaged in research and development c motor and motor drive systems for electrical vehicle. Since 199 he has been working for a Ph.D. degree in electrical engineerin in KAIST, Daejeon, Korea. His current research interests are i the areas on power electronics in automotive, such as X-by-wir ac machine drives, and DSP-based control applications in hars circumstances.

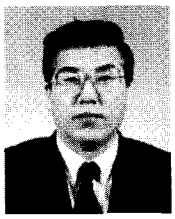

Myung-Joong Youn was born in Seou Korea on November 26, 1946. He receive the B.S. degree from Seoul Nation University, Seoul, Korea in 1970 and th M.S. and Ph.D. degrees in electric engineering from the University of Missouri Columbia in 1974 and 1978, respectively. H was with the Aircraft Equipment Division of General Electri Company at Erie, Pennsylvania, since 1978, where he was a Individual Contributor on Aerospace Electrical Engineering. H has been with the Korea Advanced Institute of Science an Technology since 1983 where he is now a professor. Hi research activities are in the areas on power electronics an control, which include the drive system, rotating electric machine design, and high performance switching regulators. Pro Youn is a member of the KIPE, KIEE, and IEEK.